

## Research Paper

# Determination of the Surface Free Energy of Crystalline and Amorphous Lactose by Atomic Force Microscopy Adhesion Measurement

Jianxin Zhang,<sup>1</sup> Stephen Ebbens,<sup>1</sup> Xinyong Chen,<sup>2</sup> Zheng Jin,<sup>1</sup> Shen Luk,<sup>1</sup> Claire Madden,<sup>1</sup> Nikin Patel,<sup>1,3</sup> and Clive J. Roberts<sup>1,2</sup>

Received August 26, 2005; accepted October 17, 2005

**Purpose.** This study was conducted to accurately measure the dispersive surface free energy of lactose solids in ordered and disordered states.

**Methods.** Atomic force microscopy (AFM) was used to determine the contact adhesion force between an AFM tip and lactose under low humidity (ca. 1% RH). The geometry of the tip contacting apex was characterized by scanning a porous aluminum film with ultrasharp spikes (radius 2–3 nm). A sphere vs. flat surface model was employed to relate the adhesion force determined to the surface energy based upon the Johnson–Kendal–Roberts theory. Spray-dried amorphous lactose in a compressed-disk form and single crystals of  $\alpha$ -lactose monohydrate were prepared as model samples.

**Results.** The condition of the smooth sample surface and sphere-shaped tip used was shown to be appropriate to the application of the JKR model. The surface energy of crystalline [(0, -1, -1) face] and amorphous lactose was determined to be  $23.3 \pm 2.3$  and  $57.4 \pm 7.9$  mJ m<sup>-2</sup>, respectively.

**Conclusions.** We have demonstrated the capability of AFM to measure the dispersive surface free energy of pharmaceutical materials directly through a blank probe at the nanometer scale. These data, although consistent with results from more traditional methods, illustrate some unique attributes of this approach, namely, surface energies are directly derived from solid–solid interactions, measurements may be made on specific crystalline faces, and the potential exists to identify the submicron heterogeneity of organic solids in terms of their molecular energy states (such as ordered and disordered lactose).

**KEY WORDS:** amorphous lactose; atomic force microscopy (AFM); crystalline lactose; solid–solid interactions; surface force measurement; surface free energy.

## INTRODUCTION

The phenomenon of solid–solid surface contacts is an important consideration in pharmaceutical processing and formulation development. One of the most important quantities that characterizes the strength of this surface contact is the surface free energy ( $\gamma$ ) of solids. This parameter can be closely related to adhesion between two surfaces brought into contact. Therefore knowledge of the solid surface energy is very useful in predicting and modeling the interactive behavior between different components in solid dosage formulation (1,2). For example, in a dry powder inhalation (DPI) preformulation, the surface energies of drug particles, excipient carriers, and packaging material can be used to predict the interaction strength between each pair of these ingredients and thus to determine the suitability of the combination (1–6).

Conventional methods used to determine the surface free energy include contact angle measurement and inverse gas

chromatography (IGC) (7,8). The experimental determination of  $\gamma$  based upon measuring the contact angle of liquid probes with known surface energies on solids using Young's equation (7) is straightforward for flat, homogeneous, and inert macroscopic samples. However, problems are encountered when samples are rough, porous, or sensitive to the liquid probes (8). Second, the technique records the average surface properties of heterogeneous surfaces due to its lack of spatial resolution. In addition, in practice the  $\gamma$  value determined depends on the combination of liquids used (9). IGC helps to overcome such limitations for powder samples; however, it is believed to preferentially probe the highest energy sites (10), reducing its ability to fully characterize a material. Therefore, there is a growing interest in seeking alternative methods to overcome these problems. In particular, new techniques are also needed to meet the current trend for examination of surfaces with defined microscale (12) or nanoscale (13,14) characteristics.

Recently, atomic force microscopy (AFM) was used to determine the surface energy of pharmaceutical materials from adhesion force measurements (1–6). The principle of AFM surface force measurements or force–distance measurements is well described in literature. Briefly, the adhesion or pull-off force ( $F$ ) is defined as the force required to pull the tip off a substrate surface. It is calculated from Hooke's law,  $F = K\Delta x$ , where  $K$  is the spring constant of cantilever and  $\Delta x$  is the

<sup>1</sup> Molecular Profiles Ltd., 8 Orchard Place, Nottingham Business Park, Nottingham, NG8 6PX, UK.

<sup>2</sup> Laboratory of Biophysics and Surface Analysis, School of Pharmacy, University of Nottingham, Nottingham, NG7 2RD, UK.

<sup>3</sup> To whom correspondence should be addressed. (e-mail: npatel@molprofiles.co.uk)

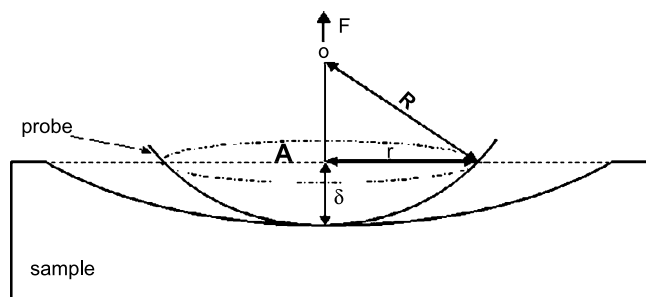


**Fig. 1.** Schematic of a spherical tip in contact with deformable surface.  $R$  is the AFM tip radius,  $r$  is the radius of a circular plane at the cross-section of the tip when the sample deforms to its maximum extent,  $A$  is the area of the circular plane, and  $\delta$  is the sample deformation.

maximum deflection of the cantilever during tip-sample contact. With proper calibration and AFM setups, these two parameters, and therefore  $F$ , can be obtained with good accuracy. In this method, the probe is normally functionalized with a particulate sample or colloid particle that is challenged against a flat surface (4,5) or sample material (1,2,5). The forces measured can be directly used to qualitatively compare the adhesion properties of the samples or quantitatively after normalization of the contacting surface area (3).

In this work, we accurately measure the dispersive component of the surface free energy of two important pharmaceutical materials using an AFM bare probe approach as opposed to the particle-functionalized probe method. These materials are crystalline  $\alpha$ -monohydrate lactose and spray-dried amorphous lactose, as widely used as excipients in a range of dosage forms. They have also been the subject of previous investigations with well-characterized surface properties (10,11), therefore offering the possibility of a direct comparison with the current study.

## BACKGROUND THEORY

**Adhesion Force vs. Surface Free Energy.** In AFM force measurements, continuum contact mechanics models are used to analyze the pull-off force. A sphere in contact with a flat substrate is generally used as a model. Based upon the Hertz theory, two contact mechanics models—Johnson–Kendall–Roberts (JKR) (15) and Deryaguin–Muller–Toporov (DMT) (16)—are frequently employed. The difference between these models is that the former assumes that surface attractive forces act only inside the particle–substrate contact region, whereas the latter assumes the attractive forces operate outside the contact region. Following previous arguments (17), JKR is considered here to be the most suitable model to derive the surface energy. This model correlates the pull-off (adhesion) force ( $F$ ) with work of adhesion ( $W_A$ ) through the following analytical equation.

$$F = \frac{3}{2} \pi R W_A \quad (1)$$

where  $R$  is the radius of the sphere (probe tip). The work of adhesion can be calculated by using Eq. (2) (15).

$$W_A = 2\sqrt{\gamma_1 \gamma_2} \quad (2)$$

where  $\gamma_1$  and  $\gamma_2$  are the dispersive components of the surface energy of the probe tip and sample lactose.  $\gamma_1$  was taken to be

$42 \text{ mJ m}^{-2}$  for the silica tip (18,19). Note that the surface free energy in the present study refers to the dispersive component of the total surface free energy, which is mainly contributed from Lifshitz–van der Waals (LW) forces. However, AFM normally measures the sum of all forces interacted between the tip and sample, which may include capillary, electrostatic, and LW forces. Here, electrostatic and capillary forces have been minimized by carrying out the experiments at low humidity (1% RH) and by removing electrostatic charges before the samples prior to force data collection. No effects due to subsequent tribocharging were observed.

Combining Eqs. (1) and (2) derives:

$$\gamma_2 = \left( \frac{F}{3\pi R} \right)^2 \frac{1}{\gamma_1} \quad (3)$$

The unknown,  $F$ , is measured by AFM force measurement and the other unknown,  $R$ , is derived as follows.

**Determination of Tip Radius.** Figure 1 schematically shows a deformation ( $\delta$ ) induced in the sample surface when a load is applied through the cantilever tip. It is assumed that  $\delta$  is generated purely from the sample deformation, and the strain induced to the tip under the load is negligible as the modulus of the silica is significantly higher than organic materials. We also assume that the shape of the tip apex is spherical at the nanoscale.

As shown in Fig. 2,  $\delta$  can be measured by collecting an AFM force–distance curve on a stiff silicon wafer surface under the same conditions. In this measurement, it is assumed that there is no depth penetration in the rigid wafer. The tip radius ( $R$ ) can then be calculated by:

$$R = \frac{r^2 + \delta^2}{2\delta} \quad (4)$$

where  $r$  is the radius of a circular plane at the cross-section of the tip when the sample deforms to its maximum extent (Fig. 1). Equation (4) can then be rearranged as:

$$R = \frac{A + \pi\delta^2}{2\pi\delta} \quad (5)$$

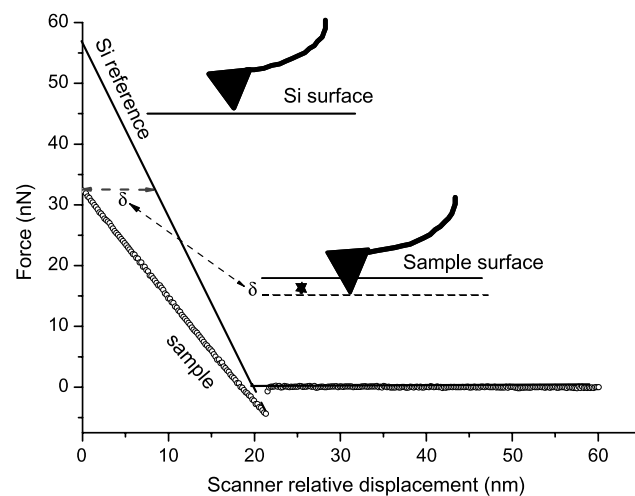


**Fig. 2.** An example AFM force–distance curves recorded against a lactose sample and a silicon reference and the method used to determine the sample deformation.

where  $A$  is the cross-section area of the tip when the sample deforms at its maximum strain and can hence be determined when  $\delta$  is known.

## MATERIALS AND METHODS

**Materials.** Alpha monohydrate lactose (Respirose SV001 from DMV, Veghel, Netherlands) was spray-dried from a 10% w/v solution using a Buchi minispray drier 190 with an inlet temperature of 166°C, an outlet temperature of 97°C, and a flow rate of 13 mL min<sup>-1</sup> to generate an amorphous sample. The spray-dried lactose was proved to be amorphous using powder X-ray diffraction (Philips X-pert Diffractometer). This material was stored under a phosphorous pentoxide desiccant prior to analysis. To facilitate AFM data acquisition from the spray-dried amorphous lactose, the sample was prepared in a disk form by pressing the sample powders into a die (Specadie, Specac Ltd., Kent, UK). The disk formed is approximately 8 mm in diameter and 1 mm thick. Infrared analysis (Smart Golden Gate, Avatar 370 FT-IR, Thermo Nicolet, Madison, WI, USA) indicated that the sample disk preparation did not affect the physical state of the amorphous lactose.

The same  $\alpha$ -lactose monohydrate was also recrystallized according to a solvent evaporation method (1) to produce a smooth surface crystalline for force measurements. Samples were analyzed as prepared. It was found that the crystals made intimate contact with the glass slide, and so were rigidly supported during force distance measurements. The dominant crystal morphology was prismatic with the largest and hence most accessible face being the (0, -1, -1) face (20). All the samples were scanned with Static Line II (Agar Scientific, Stansted, UK) to remove possible electrostatic charges before they were subjected to the force distance acquisition.

**Adhesion Force Measurement.** Adhesion force was measured using an EnviroScope AFM (Veeco, Santa Barbara, CA, USA) equipped with a Nanoscope IV controller and an environment chamber. The measurements were performed at ambient temperature ( $\sim 24^\circ\text{C}$ ) and a humidity that was controlled to be lower than 1% RH. The low humidity was generated by constantly supplying the EnviroScope sample chamber with dried air. The temperature and humidity were simultaneously monitored with a HygroPalm hygrometer (Rotronic, Huntington, NY, USA). Ten and sixteen force measurements were made for the amorphous and crystal lactose, respectively, with the same cantilever and experimental parameters. A distance of 200 nm was set between sampling points. Following the sample characterization, force curves were also immediately collected against a freshly cleaned silicon wafer, which was used as a nonindenting reference to determine the sample deformation. The silicon wafer surface was cleaned using a Piranha solution [mixture of 30% H<sub>2</sub>O<sub>2</sub> and 70% concentrated H<sub>2</sub>SO<sub>4</sub> (1:4)] at ambient temperature. The treated silicon was then rinsed with Millipore water, ethanol, and finally dried in a stream of nitrogen gas.

FESP probes (Veeco) were used to collect force-distance data. The spring constant of the FESP probe used was measured to be 2.05 N m<sup>-1</sup> using Sader *et al.*'s method (21). Prior to data collection, the probes were cleaned using a UV tip cleaner (Bioforce Nanosciences, Ames, IA, USA) for

20 min to remove organic contaminants on the probe surface. Such a procedure also resulted in oxidation of the silicon on the probe surface (22). A number of published work have shown that the dispersive surface energy of silica ( $\gamma_1$ ) determined using contact angle technique ranges approximately from 41 to 43 mJ m<sup>-2</sup> (18,19). We took silica  $\gamma_1$  to be 42 mJ m<sup>-2</sup> in this study. As shown in Fig. 2, the sample surface deformation ( $\delta$ ) due to indentation was calculated from the difference in gradient of the force-distance approach curve subsequent to contact between the reference and sample surface.

**Tip Geometry Characterization.** The tip radius of the probe was characterized by tip self-imaging, whereby a tip rather, than the sample, is imaged when the dimensions of surface features of the sample are similar or sharper than that of the probe. To do this, the tip was scanned across a thin film of porous Aluminum (PA01, Agar Scientific) within a 500 × 500 nm area at 2 Hz. The film consists of hexagonal

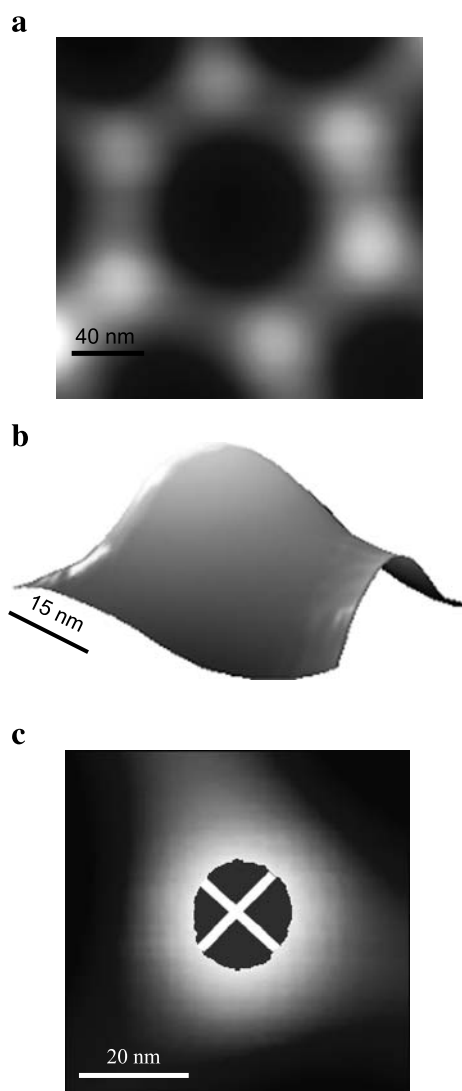


**Fig. 3.** (a) Repeated tip images caused by scanning from a porous aluminum film with spikes distributed hexagonally. (b) Three-dimensional representation of one of the tip self-images. (c) The highlighted area is the cross-sectional area ( $A$ ) of the tip when the sample surface deforms to a maximum extent.

hollow cells formed by vertical partitions. The curvature radius of the spikes formed at the intersections of the partitions is claimed to be 2–3 nm. A noncontact or tapping mode (DI Multimode Nanoscope III, Veeco) was employed to image the tip using this film. During the imaging, the set-point was set as high as possible, to reduce the interactions between the tip and the aluminum, and therefore possible damage to the tip. The image generated is in fact a convolution of the tip and sample surface features; however, it predominantly describes the tip profile as the spikes are much sharper (Figs. 3a and b). The highlighted region in Fig. 3c represents the area,  $A$ , as detailed in Eq. (5) and Fig. 1. The value of  $A$  and that of  $\delta$  were used to determine the tip radius,  $R$ .

Scanning electron microscopy (SEM) was carried out on the sample surfaces using a Leo 1430 VP electron microscope. The accelerating voltage used was 3–7 kV at a working distance of 9 mm.

## RESULTS

Prior to AFM force measurements, the surface of the crystalline lactose and the compressed amorphous disk were examined by SEM. Figure 4 shows that the surface topographies of these two samples are very smooth in general. This

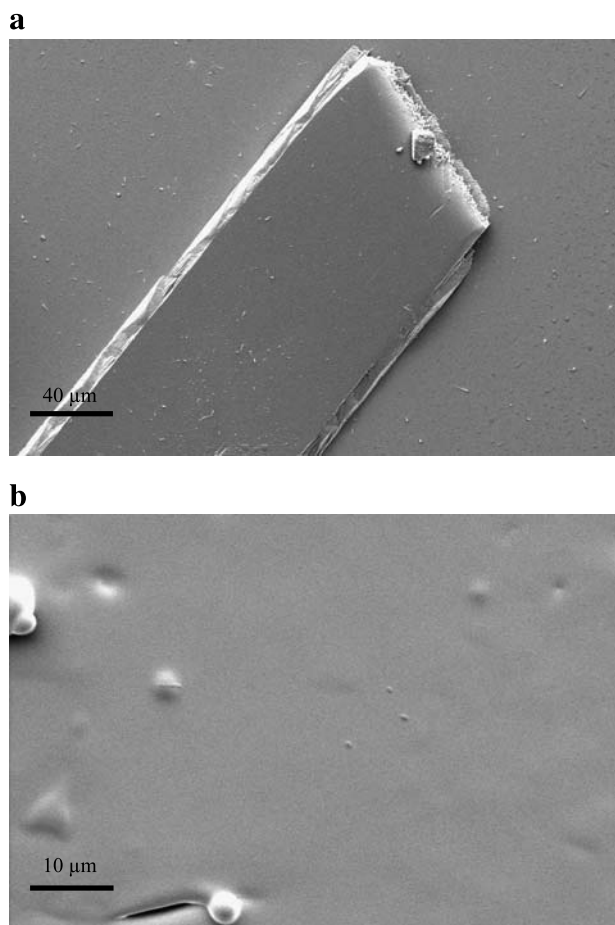


**Fig. 4.** SEM micrographs of (a) the surface of a recrystallized  $\alpha$ -monohydrate lactose single crystal and (b) a compressed disk of spray-dried amorphous lactose, showing the surfaces of these two samples are locally smooth.

is consistent with our intention to create a smooth sample surface. Although a small degree of surface imperfections exist in localized regions on the amorphous sample (Fig. 4b), these can be avoided with the aid of an optical microscope attached onto the AFM. Therefore it is always possible to select smooth regions to minimize a possible effect of surface roughness to the accurate determination of the surface energy. We have quantitatively assessed the surface roughness by AFM. The mean root mean square (RMS) roughness was recorded to be 0.44 nm within a  $2 \times 2 \mu\text{m}$  area for the crystal. For the amorphous sample, the level of surface smoothness (RMS = 0.36 nm) was similar within the same area. Figure 4a also demonstrates that the force data was collected solely from the dominant (0, -1, -1) face of the prismatic  $\alpha$ -lactose monohydrate crystal (20).

As stated, the data in Figs. 3a and b illustrate the apex profile of the AFM tip imaged with the ultrasharp spikes. These images demonstrate that the tip apex of the probe approximates to a sphere at the nanoscale, consistent with our use of a sphere plane model geometry.

Figure 5 presents typical force distance curves for both crystalline and amorphous lactose samples. It shows that the maximum load applied in pushing the tip into contact with the sample surface was approximately 30 nN. This load level applies to both samples. However, the adhesion force in pulling the probe from the sample was different for the crystalline and amorphous surfaces. The average pull-force measured was  $6.34 \pm 0.35$  nN for the crystal and  $10.01 \pm 0.80$  nN for the glassy lactose (Table I). Although contact area effects due to different indentation depths must be clearly taken into account (as below), these results demonstrate that the conformation and order of the lactose molecules affects the magnitude of the adhesion force on the surface with the disordered surfaces displaying approximately 35% stronger adhesion than the ordered surface. Figure 5 also suggests that both the crystalline and amorphous samples deformed within an elastic limit as the approach and retract curves almost completely overlap within the contact region. The  $\delta$  for the crystal surface was determined to be  $2.3 \pm 0.1$  nm. For the disordered lactose, the value was slightly higher with  $2.6 \pm 1.0$

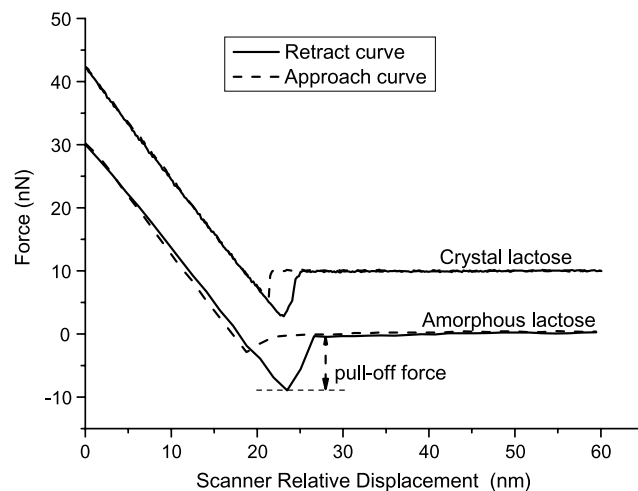


**Fig. 5.** Comparison of the force–distance curves of the crystalline lactose with those of the amorphous lactose. For clarity, the force data from the crystal was deliberately shifted away from the level position.

**Table I.** Surface Free Energy of the Crystalline and Amorphous Lactose Samples, Pull-Off Forces and Sample Deformation Measured

	Pull-Off Force, $F$ (nN)	Sample Deformation, $\delta$ (nm)	Surface Energy, $\gamma_2$ (mJ m <sup>-2</sup> )
Crystalline lactose	6.34 ± 0.35	2.33 ± 0.11	23.3 ± 2.3
Amorphous lactose	10.01 ± 0.80	2.61 ± 0.96	57.4 ± 7.9

Surface energy of silicon oxide:  $\gamma_1 = 42$  mJ m<sup>-2</sup> (18,19).  
Spring constant determined:  $K = 2.05$  N m<sup>-1</sup>.

nm, in agreement with the fact that the amorphous sample would be expected to be less rigid than the crystal. Subsequently, the cross-section area (Fig. 3c) of the tip at the maximum deformation of the sample was determined based upon the  $\delta$  value. These two parameters were then fitted into a circle describing the radius of the curvature of the tip apex in contact with the sample. The tip radius calculated using Eq. (5) was  $21.6 \pm 0.6$  nm, which is in agreement with the nominal range supplied by the manufacture (it should be noted that as  $\delta$  is significantly smaller than  $R$ , the radius of curvature of the deformed sample is assumed negligible and therefore does not enter the calculation of  $\gamma$ ). Hence, according to Eq. (3), the surface free energy ( $\gamma_2$ ) determined was  $23.3 \pm 2.3$  mJ m<sup>-2</sup> for the crystal and  $57.4 \pm 7.9$  mJ m<sup>-2</sup> for the amorphous lactose (Table I).

## DISCUSSION

The molecular order of crystalline lactose is disrupted in producing amorphous or glassy lactose during the spray-drying process. In doing so, energy is supplied for this molecular disruption to generate the amorphous form. It is not unexpected in this study that the amorphous lactose has a higher surface free energy than its crystalline counterpart, as the former is disordered and thus is in a higher energy state, which can be thermodynamically unstable. Previously, the same trend was also reported using IGC and contact angle measurement (10,11) (see Table II).

As a definition, surface free energy is the energy required to create a unit area of surface *in vacuo*. In practice, it is difficult to pursue and measure the absolute surface

**Table II.** Comparison of the values of Surface Energy (Dispersive Component) determined from AFM Force Measurement in the present study with those from IGC and Surface Contact Angle Measurement in literature

	AFM	IGC	Contact Angle (°)
Crystalline lactose (mJ m <sup>-2</sup> )	23.3	41.4 (8)	7–43 (9)
		39.3 (10)	24.6 (10)
		31.2 (11)	27.8 (24)
			43.5 (25)
Amorphous lactose (mJ m <sup>-2</sup> )	57.4	41.4 (10)	29.5 (10)
		37.1 (11)	

energy of a substance (23). As shown in Table II, the measured  $\gamma$  value of  $\alpha$ -monohydrate lactose varies from 7 to 43 mJ m<sup>-2</sup> from different laboratories (9,10,24,25) using the contact angle technique. In this study, the real  $\gamma_2$  values of the crystal and amorphous lactose may be smaller than calculated, because the radius of the curvature of the sample surface after the stress recovery may not be infinite (26). It is, however, believed that the margin affected should be small as the samples deformed elastically at their maximum strain as suggested in Fig. 5. In addition, the parameters of the surface energy obtained from different methods cannot be easily compared, because the theoretical approach used to derive the quantity and the nature of the test is different. IGC is used to determine solid–vapor interactions and a higher  $\gamma$  value from high-energy sites due to infinite dilution is normally obtained; whereas contact angle measurement is based upon solid–liquid interactions and the derived  $\gamma$  represents the average. For the current approach, solid–solid interactions are used to derive the dispersive contribution to the surface energy. Therefore it is not surprising to find that the  $\gamma$  values determined with the AFM are in general close to those from the above two techniques, but not identical. It may be appropriate to apply these three methods in different situations. The current method may be more applicable to study solid–solid interactions as required, for example, by DPI development where the interactions of drugs, carriers, and container materials are the main concern and where little material is available.

One distinctive point observed in the AFM method is that there is a substantial difference between the  $\gamma$  of the crystalline ( $23.3$  mJ m<sup>-2</sup>) and the amorphous ( $57.4$  mJ m<sup>-2</sup>) lactose in comparison with the difference obtained from other methods (10,11). This is partly a result of the sensitivity of the approach, but is primarily attributable to the ability of AFM to effectively isolate the surface energy of a single crystal face, in this case the dominant lowest energy face. Hence, this provides the largest separation in surface energies one would expect between the crystalline and the amorphous material. Techniques such as contact angle, which produces an average energy measurement generally, reveal values between this lower and upper limit, whereas IGC, which is biased toward measurement of high-energy sites, yields values for crystalline lactose very close to the amorphous value. This observation suggests that AFM, with further development, could have a role in identifying the presence of polymorphism or amorphous material in formulation and pharmaceutical manufacture processes such as milling, particle size reduction, and compression (13). In addition to this nanoscale  $\gamma$  characterization, a possibility exists to map variations in  $\gamma$  on a surface. This combined capability would be similar to proposed applications of scanning thermal microscopy (12) or AFM phase imaging (14), although with much higher spatial resolution than the former and more quantitative than the latter.

In Table I, it is clear that the variation of the force value determined in this study is approximately 6%, which is generally much lower than previously reported in the literature (4,5). One reason for this is that the RMS roughness of the samples was low (0.36–0.44 nm), which reduces fluctuations in contact area and hence  $F$ . Other contributors are that the surface of both the crystal and

amorphous samples used here are homogeneous and that the accuracy of  $F$  measurement is very high ( $\pm 10$  pN). The major contributors to the errors observed here are in fact linked to the accuracy of the spring constant  $K$  calibration ( $\pm 5\%$ ) and the determination of  $R$  (ca. 3%), both areas where improvements might soon be expected (27,28). In the specific case of amorphous content, it is interesting to speculate on the level of sensitivity of AFM (assuming that such amorphous material is likely to be at a surface) in comparison to conventional approaches, which currently are at best around 1%. Clearly, as each individual force measurement from a nanoscale area is potentially capable of identifying the presence of amorphous material, the question is not one of sensitivity but of the time needed to randomly challenge such an area with an AFM probe. For samples amenable to AFM analysis, we estimate that achieving better than a 1% sensitivity would take on the order of hours.

Finally, the ability to accurately determine surface energies from individual crystal faces clearly raises the possibility of comparing such data from that produced through molecular modeling (29,30), perhaps allowing the refinement of such theoretical approaches to crystal morphology prediction.

## CONCLUSIONS

Building upon previous work, a refined approach to measuring the surface free energy (ascribed principally to the dispersive component) of solids was developed using AFM force measurement. The method allows the surface free energy of pharmaceutical materials to be determined through solid–solid interactions at the nanoscale. The surface energy determined from a single crystal [(0, -1, -1) face] of  $\alpha$ -lactose monohydrate was  $23.3 \pm 2.3$  mJ m<sup>-2</sup> and for the amorphous form  $57.4 \pm 7.9$  mJ m<sup>-2</sup>. These values, although consistent with those obtained from inverse gas chromatography and contact angle measurement, much more clearly delineate the crystalline and amorphous forms of lactose. In addition, the AFM data indicate new opportunities for material characterization. Finally contact angle approaches produce an average energy measurement and IGC is biased toward measurement of high-energy sites, AFM provides access to localized measurements, say from individual faces or in the identification and localization of components within heterogeneous samples (e.g., surface amorphous material within a crystalline sample).

## ACKNOWLEDGMENT

We thank Mrs S. Evans for assistance in sample preparation and SEM analysis.

## REFERENCES

1. P. Begat, D. A. V. Morton, J. N. Staniforth, and R. Price. The cohesive–adhesive balances in dry powder inhaler formulations. I. Direct quantification by atomic force microscopy. *Pharm. Res.* **21**:1591–1597 (2004).
2. M. D. Louey, P. Mulvaney, and P. J. Stewart. Characterisation of adhesional properties of lactose carriers using atomic force microscopy. *J. Pharm. Biomed. Anal.* **25**:559–567 (2001).
3. C. J. Roberts. What can we learn from atomic force microscopy adhesion measurements with single drug particles? *Eur. J. Pharm. Sci.* **24**:153–157 (2005).
4. J. C. Hooton, C. S. German, S. Allen, M. C. Davies, C. J. Roberts, S. J. B. Tendler, and P. M. Williams. An atomic force microscopy study of the effect of nanoscale contact geometry and surface chemistry on the adhesion of pharmaceutical particles. *Pharm. Res.* **21**:953–961 (2004).
5. M. Davies, A. Brindley, X. Chen, M. Marlow, S. W. Doughty, I. Shrubbs, and C. J. Roberts. Characterization of drug particle surface energetics and Young's modulus by atomic force microscopy and inverse gas chromatography. *Pharm. Res.* **22**:1158–1166 (2005).
6. V. Berard, E. Lesniewska, C. Andres, D. Pertuy, C. Laroche, and Y. Pourcelot. Affinity scale between a carrier and a drug in DPI studied by atomic force microscopy. *Int. J. Pharm.* **247**:127–137 (2002).
7. A. W. Neumann and R. J. Good. In R. J. Good and R. D. Stromberg (eds.), *Surface and Colloid Science*, Vol. 11, Plenum, New York, 1979, p. 31.
8. I. M. Grimsey, J. C. Feeley, and P. York. Analysis of the surface energy of pharmaceutical powders by inverse gas chromatography. *J. Pharm. Sci.* **91**:571–583 (2002).
9. O. Planinsek, A. Trojak, and S. Srčić. The dispersive component of the surface free energy of powders assessed using inverse gas chromatography and contact angle measurements. *Int. J. Pharm.* **221**:211–217 (2001).
10. N. M. Ahfat, G. Buckton, R. Burrows, and M. D. Ticehurst. An exploration of inter-relationships between contact angle, inverse phase gas chromatography and triboelectric charging data. *Eur. J. Pharm. Sci.* **9**:271–276 (2000).
11. H. E. Newell, G. Buckton, D. A. Butler, F. Thielmann, and D. R. Williams. The use of inverse phase gas chromatography to measure the surface energy of crystalline, amorphous, and recently milled lactose. *Pharm. Res.* **18**:662–666 (2001).
12. J. X. Zhang, C. J. Roberts, K. M. Shakesheff, M. C. Davies, and S. J. B. Tendler. Micro- and macrothermal analysis of a bioactive surface-engineered polymer formed by physical entrapment of poly(ethylene glycol) into poly(lactic acid). *Macromolecules* **36**:1215–1221 (2003).
13. S. Ward, M. Perkins, J. X. Zhang, C. J. Roberts, C. E. Madden, S. Luk, N. Patel, and S. J. Ebbens. Identifying and mapping surface amorphous domains. *Pharm. Res.* **22**:1195–1202 (2005).
14. J. X. Zhang, A. J. Busby, C. J. Roberts, X. Y. Chen, M. C. Davies, S. J. B. Tendler, and S. M. Howdle. Preparation of a poly(methyl methacrylate)/ultrahigh molecular weight polyethylene blend using supercritical carbon dioxide and the identification of a three-phase structure: an atomic force microscopy study. *Macromolecules* **35**:8869–8877 (2002).
15. K. L. Johnson, K. Kendall, and A. D. Roberts. Surface energy and the contact of elastic solids. *Proc. R. Soc. Lond.* **A324**:301–313 (1971).
16. B. V. Derjaguin, V. M. Muller, and Y. P. Toporov. Effect of contact deformations on the adhesion of particles. *J. Colloid Interface Sci.* **53**:314–326 (1975).
17. J. C. Hooton, C. S. German, S. Allen, M. C. Davies, C. J. Roberts, S. J. B. Tendler, and P. M. Williams. Characterisation of particle–interactions by atomic force microscopy: the effect of contact area. *Pharm. Res.* **20**:508–514 (2003).
18. E. Chibowski and R. Perea-Carpio. Problems of contact angle and solid surface free energy determination. *Adv. Colloid Interface Sci.* **98**:245–264 (2002).
19. M. L. Gonzalez-Martin, B. Janczuk, L. Labajos-Broncano, J. M. Bruque, and C. M. Gonzalez-Garcia. Analysis of the silica surface free energy by the imbibition technique. *J. Colloid Interface Sci.* **240**:467–472 (2001).
20. T. D. Dincer, G. M. Parkinson, A. L. Rohl, and M. I. Ogden. Crystallisation of  $\alpha$ -lactose monohydrate from dimethyl sulfoxide (DMSO) solutions: influence of  $\beta$ -lactose. *J. Cryst. Growth* **205**:368–374 (1999).
21. J. E. Sader, J. W. M. Chon, and P. Mulvaney. Calibration of rectangular atomic force microscope cantilevers. *Rev. Sci. Instrum.* **70**:3967–3969 (1999).

22. W. Kern. *Handbook of Semiconductor Wafer Cleaning Technology: Science, Technology and Applications*, Noyes Publications, Park Ridge, NJ, 1993.
23. J. Drelich, G. W. Tormoen, and E. R. Beach. Determination of solid surface tension from particle-substrate pull-off forces measured with the atomic force microscope. *J. Colloid Interface Sci.* **280**:484–497 (2004).
24. X. Pepin, S. Blanchon, and G. Couarraze. Powder dynamic contact angle measurements: young contact angles and effectively wet perimeters. *Powder Technol.* **99**:264–271 (1998).
25. F. Podczek. Investigations into the reduction of powder adhesion to stainless steel surfaces by surface modification to aid capsule filling. *Int. J. Pharm.* **178**:93–100 (1999).
26. F. Podczek, J. M. Newton, and M. B. James. The estimation of the true area of contact between microscopic particles and a flat surface in adhesion contact. *J. Appl. Phys.* **79**:1458–1463 (1996).
27. P. J. Cumpson, J. Hedley, and P. Zhdan. Accurate force measurement in the atomic force microscope: a microfabricated array of reference springs for easy cantilever calibration. *Nanotechnology* **14**:918–924 (2003).
28. J. H. Hafner, C.-Li Cheung, T. H. Oosterkamp, and C. M. Lieber. High-yield assembly of individual single-walled carbon nanotube tips for scanning probe microscopies. *J. Phys. Chem. B* **105**:743–746 (2001).
29. G. Clydesdale, K. J. Roberts, G. B. Tefler, and J. W. Grant. Modeling of crystal morphology of  $\alpha$ -lactose monohydrate. *J. Pharm. Sci.* **86**:135–141 (1997).
30. T. H. Muster and C. A. Prestidge. Face specific surface properties of pharmaceutical crystals. *J. Pharm. Sci.* **91**:1432–1444 (2002).